Disease Expression of *RP1* Mutations Causing Autosomal Dominant Retinitis Pigmentosa

Samuel G. Jacobson,[1] *Artur V. Cideciyan,*[1] *Alessandro Iannaccone,*[1,6] *Richard G. Weleber,*[2] *Gerald A. Fishman,*[3] *Albert M. Maguire,*[1] *Louisa M. Affatigato,*[4] *Jean Bennett,*[1] *Eric A. Pierce,*[1] *Michael Danciger,*[5] *Debora B. Farber,*[5] *and Edwin M. Stone*[4]

Purpose. To determine the disease expression in heterozygotes for mutations in the *RP1* gene, a newly identified cause of autosomal dominant retinitis pigmentosa (adRP).

Methods. Screening strategies were used to detect disease-causing mutations in the *RP1* gene, and detailed studies of phenotype were performed in a subset of the detected *RP1* heterozygotes using electroretinography (ERG), psychophysics, and optical coherence tomography (OCT).

Results. Seventeen adRP families had heterozygous *RP1* changes. Thirteen families had the Arg677ter mutation, whereas four others had one of the following: Pro658 (1-bp del), Ser747 (1-bp del), Leu762-763 (5-bp del), and Tyr1053 (1-bp del). In Arg677ter *RP1* heterozygotes, there was regional retinal variation in disease, with the far peripheral inferonasal retina being most vulnerable; central and superior temporal retinal regions were better preserved. The earliest manifestation of disease was rod dysfunction, detectable as reduced rod ERG photoresponse maximum amplitude, even in heterozygotes with otherwise normal clinical, functional, and OCT cross-sectional retinal imaging results. At disease stages when cone abnormalities were present, there was greater rod than cone dysfunction. Patients with the *RP1* frameshift mutations showed similarities in phenotype to those with the Arg677ter mutation.

Conclusions. Earliest disease expression of *RP1* gene mutations causing adRP involves primarily rod photoreceptors, and there is a gradient of vulnerability of retinopathy with more pronounced effects in the inferonasal peripheral retina. At other disease stages, cone function is also affected, and severe retina-wide degeneration can occur. The nonpenetrance or minimal disease expression in some Arg677ter mutation-positive heterozygotes suggests important roles for modifier genes or environmental factors in *RP1*-related disease. (*Invest Ophthalmol Vis Sci.* 2000;41:1898–1908)

A novel gene associated with autosomal dominant retinitis pigmentosa (adRP) was recently identified.[1–3] This represents the fourth gene associated with adRP; the others are *rhodopsin* (*RHO*), *peripherin/retinal degeneration slow* (*RDS*), and *neural retina leucine zipper* (*NRL*).[4,5] Subsequent reports have further explored the *RP1* gene and expanded the spectrum of mutations known to cause RP,[6,7] but detailed studies of disease expression have not been reported.

We identified heterozygous mutations in the *RP1* gene in a large cohort of patients with RP and then studied the disease phenotype associated with the most commonly found mutation, arginine-677-ter (Arg677ter) and with four other frameshift mutations. Knowledge of the disease expression should increase understanding of the pathophysiology of *RP1*-related human retinal degeneration and provide a set of human findings to serve as a standard for comparison with future in vitro results and animal models of this relatively common form of adRP.

Methods

Subjects

A total of 1941 probands with the clinical diagnosis of RP (who had been screened previously for coding sequence mutations in *RHO* and *RDS* genes and found to be negative) were included in this study. The probands included patients with simplex, multiplex, autosomal recessive, or autosomal dominant forms of RP. All patients were involved in the molecular studies; a subset was investigated for phenotype. A multigeneration kindred with adRP and the Arg677ter mutation in the *RP1* gene was part of this series.[3] Ninety-five unrelated individuals without eye disease were also included as control subjects in the molecular studies. Subjects gave informed consent after explanation of the procedures. Research procedures were in accordance with institutional guidelines and the Declaration of Helsinki.

From the [1]Department of Ophthalmology, Scheie Eye Institute, University of Pennsylvania, Philadelphia; [2]Casey Eye Institute, Oregon Health Sciences University, Portland; [3]Department of Ophthalmology, University of Illinois College of Medicine, Chicago; [4]University of Iowa Hospitals and Clinics, Iowa City; [5]Jules Stein Eye Institute, University of California Los Angeles School of Medicine.

[6]Present address: Department of Ophthalmology, University of Tennessee, Memphis.

Supported by The Foundation Fighting Blindness; National Institutes of Health Grants EY-05627, EY-10539, EY-08426, EY-08285, and EY-02651; The Daniel Matzkin Research Fund; The Chatlos Foundation; the Grousbeck Family Foundation; the Carver Charitable Trust; the F. M. Kirby Foundation; and the Mackall Trust.

Submitted for publication November 18, 1999; revised January 18, 2000; accepted February 2, 2000.

Commercial relationships policy: N.

Corresponding author: Samuel G. Jacobson, Scheie Eye Institute, 51 N. 39th Street, Philadelphia, PA 19104. jacobsos@mail.med.upenn.edu

Molecular Analyses

The screening of the 1941 RP probands and 95 control subjects was performed in three stages. First, the entire gene was screened in 182 patients and 95 control subjects. Next, the portion of the gene encoding codons 657-896 was screened in an additional 180 patients. Finally, an additional 1579 probands were screened for the presence of the Arg677ter *RP1* mutation.

In all cases, RP patients and control subjects were screened identically, using single-strand conformational polymorphism analysis (SSCP) followed by automated bidirectional DNA sequence confirmation of the observed SSCP shifts. Screening of the entire gene required the assay of 38 different amplimers, whereas the screening of codons 657-896 required the assay of four amplimers, and the detection of the mutation at codon 677 required the assay of only one. The sequences of the oligonucleotide primer pairs (available on request) were derived from the published gene sequence (GenBank accession number AF141021).

For SSCP, 12.5 ng of each individual's DNA was used as a template in an 8.35-μl PCR containing 1.25 μl buffer (100 mM Tris-HCl [pH 8.3]; 500 mM KCl; 15 mM $MgCl_2$); 300 μM each of dCTP, dATP, dGTP, dTTP; 1 picomole of each oligonucleotide primer; and 2.5 units of polymerase [Biolase]. Samples were denatured for 5 minutes at 94°C and incubated in a DNA thermocycler (Omnigene, Teddington, UK) for 35 cycles under the following conditions: 94°C for 30 seconds, 55°C for 30 seconds, and 72°C for 30 seconds After amplification, 5 μl of stop solution (95% formamide, 10 mM NaOH, 0.05 bromophenol blue, and 0.05% xylene cyanol) were added to each sample. The amplification products were then denatured for 3 minutes at 94°C and electrophoresed on 0.4 mm nondenaturing gels (9.75 ml 37.5:1 acrylamide–bis, 3.25 ml glycerol, 32.5 ml 1× TBE, 19.5 ml ddH_2O) with a running buffer of 0.5% TBE at 25 W for 3 hours at room temperature. After electrophoresis, gels were stained with silver nitrate.[8] Samples that exhibited shifts by SSCP were bidirectionally sequenced using fluorescent dideoxynucleotides with an automated sequencer (model 377; Applied Biosystems, Foster City, CA).

Phenotype Analyses

A subset of *RP1* mutation-positive patients had clinical examinations, psychophysical testing, electroretinography, and optical coherence tomography (OCT).

Psychophysical Testing. Kinetic visual fields were tested with a Goldmann perimeter and results quantified.[9–11] Static threshold perimetry in the dark-adapted (500- and 650-nm stimuli) and light-adapted (600-nm stimulus on 10-cd/m^2 white background) states was performed using an automated perimeter (Humphrey Field Analyzer, San Leandro, CA) and analyzed for photoreceptor mediation and sensitivity losses, as described previously.[12,13] In selected patients, topography of rod and long/middle wavelength (L/M) cone sensitivity losses was summarized by mapping the frequency of occurrence of a given loss. A 3 × 3 moving average filter was applied (excluding foveal and physiological blind spot loci) before interpolating the frequency map with a cubic surface and delineating the 50th percentile contour. The process was repeated for a range of sensitivity losses and resultant contours were overlaid.[14]

Dark adaptation functions were measured with a modified automated perimeter driven by an external computer running custom software.[13–16] In brief, prebleach dark-adapted thresholds were determined after more than 1 hour of dark adaptation. A yellow (>520-nm) bleaching light (20° in diameter, centered at the retinal test locus) was delivered with Maxwellian optics using a modified fundus camera (Carl Zeiss, Thornwood, NY). In a subset of patients, a 12° inferior field locus was tested, and in others, a 34° eccentric locus (inferonasal in the field to fixation) was tested. Recovery of sensitivity was measured after retinal exposure of 7.8 log scotopic troland seconds (scot-td · sec) expected to bleach approximately 99% of the available rhodopsin. Sensitivity was tested with 650-nm stimuli initially to follow the cone limb and 500-nm stimuli later to determine the rod limb. Differences between the two sensitivities were used to determine the type of mediation at a given time after the bleach.[12]

Electroretinography. Full-field electroretinographies (ERGs) were performed according to published protocols.[13,17–20] ERG photoresponses were recorded using a red (Wratten 26; Eastman Kodak, Rochester, NY) and two blue (W47A; Eastman Kodak) flash stimuli with equipment and methodology described before.[14,21,22] The red flash (3.6 log photopic troland seconds [phot-td · sec]) was photopically matched to the higher energy blue flash (4.6 log scot-td · sec) and scotopically matched to the lower energy blue flash (2.3 log scot-td · sec). A model of phototransduction consisting of the sum of rod and cone components was used to quantify the dark-adapted waveforms.[14,22] The model has maximum amplitude and sensitivity parameters for rod and cone components. A simplex algorithm was used to estimate the four parameters by fitting the model simultaneously to the leading edges of the three recorded responses. Cone-isolated ERG photoresponses were also recorded on a rod-desensitizing 3.2 log td white background with red (W26) flash stimuli. The cone phototransduction model was fit to the leading edges of these photoresponses to estimate light-adapted cone phototransduction parameters.

Optical Coherence Tomography. Cross-sectional retinal reflectivity profiles were obtained by optical coherence tomography (OCT; Humphrey). The principles of the instrument used have been published.[23,24] Vertically oriented scans (20° in extent) crossing fixation were obtained. Longitudinal motion artifacts originating from micron-scale eye and head motion were compensated for by alignment of the longitudinal reflectivity profiles (LRPs) making up each OCT.[25–28]

Results

Mutations in the *RP1* Gene

The screening of codons 657-896 in the *RP1* gene led to the finding of 10 probands with mutations. Seven of the probands were heterozygous for the Arg677ter mutation, and three were heterozygous for each of the following changes that are predicted to cause frameshifts and lead to premature termination codons: 1-bp insertion (A) in codon 658, 1-bp deletion (A) in codon 747, and a 5-bp deletion (TAAAT) in codons 762-763. These changes were not present in 95 normal individuals. When the entire *RP1* gene was examined using SSCP analysis in 182 probands and 95 normal individuals, we detected one further frameshift mutation and 12 polymorphisms. The muta-

tion, a 1-bp deletion (T) in codon 1053, would also be expected to result in premature termination of translation. The 12 polymorphisms (and observed number of occurrences of that allele per total alleles screened) were as follows: Leu76Leu (1/554), Thr93Thr (1/554), IVS2→6T-C (8/554), Ser504Ala (2/554), Asn985Tyr (137/554), Leu1417Val (1/554), Gly1402Phe (1/554), Arg1595Gln (1/554), Ala1670Thr (115/554), Gln1725Gln (135/554), Ser1961Pro (115/554), and Cys2033Tyr (85/554). The codon 1670 and 1961 polymorphisms were found together in all 115 cases. Screening for the Arg677ter *RP1* mutation in 1579 patients with RP led to the identification of six additional probands heterozygous for this mutation, three of whom were available for study of phenotype. All probands found to have *RP1* mutations were from adRP pedigrees.

Phenotype of the Arg677ter *RP1* Mutation

Clinical characteristics of 22 heterozygotes with the Arg677ter *RP1* mutation, representing 10 pedigrees, are listed in Table 1. Eleven of the patients are from one pedigree.[3] An attempt can be made to glean some information about disease progress from these cross-sectional data. In the age range from 10 to 71 years, visual acuities were normal or only moderately impaired (no worse than 20/30). Eighteen of the 22 heterozygotes had wide expanses of kinetic visual field (arbitrarily, ≥75% of normal, measured with V-4e or IV-4e targets) at their first visit. Of the four patients with lesser extents of field, two were in the fourth decade of life and two in the sixth. Serial measurements in two patients during their fourth decade of life (family 1, P4; family 5, P1) indicated substantial loss of visual field extent over this interval. These data suggest longevity of central cone-mediated vision but variability in severity of visual field loss within and between families studied.

The pattern of results of kinetic perimetry are illustrated in Figure 1 for representative heterozygotes with the Arg677ter *RP1* mutation. There can be a normal expanse of field with these targets (Fig. 1A; family 1, P3). Detectable defects at relatively early stages were mainly in the superior and temporal peripheral fields (Fig. 1A, family 1, P10; Fig. 1B, family 3, P1). At later disease stages, other regions showed abnormalities, and there was loss of midperipheral field but retained central and peripheral islands. Serial fields over an 11-year interval in P4 of family 1 illustrate progression from a stage of superior field absolute scotoma to residual central and peripheral islands (Fig. 1D). Some patients were reduced to a central island only (family 5, P2; not shown). In all patients, pigmentary retinopathy, when present, tended to be more pronounced in the inferior and nasal retina than in other regions.

The topography of rod- and L/M cone–mediated sensitivity losses across the visual field at relatively early disease stages of *RP1* Arg677ter-associated disease is summarized using data from seven heterozygotes from family 1 (P1, P5, P7–P11). There was major intraretinal variation in sensitivities. Maps of 50th percentile contours indicate a gradient of rod dysfunction with the most vulnerable region being in the superior and temporal field and least vulnerable in the central and inferonasal fields (Fig. 2A). Cone dysfunction tended to follow that of the rods (Fig. 2B). Horizontal profiles across the central 60° of visual field for rod- and cone-mediated sensitivities illustrate the progression of visual loss in the central retina of this disease (Figs. 2C, 2D, 2E). Figure 2C shows cross-sectional data in four patients with 20/20 visual acuity. P2 (and P3, not shown) had normal rod-mediated function across the central 60° (and throughout the visual field). P7 showed normal rod function in the central 20° but a decline in function at increasing eccentricities and greater dysfunction temporally than nasally. P6 retained borderline normal rod function centrally (for a few degrees of field only) that decreased to scotoma by 10° temporally and by 30° nasally. P9 had very reduced central rod function and showed no nasotemporal difference in function. Serial data are shown for P4 separated by more than a decade (Figs. 2D, 2E). At age 32, central rod function was slightly worse than that of P6, but not as reduced as in P9. By age 43, there was further reduction in rod function (Fig. 2D), but little or no change of cone function (Fig. 2E). This suggests continued vulnerability of rod more than cone function, even at late stages of this disease.

Dark adaptation was tested in seven members of family 1 at 34° in the inferonasal field (Fig. 3A) or at 12° in the inferior field (Fig. 3B). Prebleach (PB) thresholds were normal in six patients, but P1 showed a 0.4-log unit elevation. Cone recovery (Fig. 3, insets) was normal in all patients, both in cone plateau thresholds and recovery kinetics. Early phase of the recovery kinetics of the rod limb was quantified by the cone–rod break time, and the later phase was quantified by the time to recover to within 0.5 log units of prebleach sensitivity.[14] Cone–rod break time was normal (12.5 ± 0.9 minutes) in all patients. P3 and P8 had normal (36 ± 3 minutes) late-phase kinetics, whereas P1, P2, P7, P10, and P11 had small late-phase delays, ranging from 9 to 16 minutes from mean normal.

The dark adaptation results in these patients with the Arg677ter *RP1* mutation are of interest to compare with those in the P23H *RHO* gene mutation, another common cause of adRP (Fig. 3B). Adaptation abnormalities have been found in many of the *RHO* mutations.[13–15,29] In a representative patient with the P23H *RHO* gene mutation (tested at 10° in the inferior field after 99% bleach; Fig. 3B, open circles), rod threshold was elevated by 0.45 log units, but cone plateau threshold was normal. Cone–rod break time was normal, but the late phase of rod kinetics was delayed by 114 minutes compared with mean normal.

Rod ERG b-waves and cone flicker ERGs were within normal limits for three patients (Table 1: family 1, P2 and P3; family 3, P1) but were abnormally reduced in amplitude in the other patients tested. In all cases with abnormal responses, the percentage loss of amplitude of rod b-wave was greater than that for cone flicker. Cone flicker timing could be normal or delayed. ERG photoresponses recorded in family 1 ranged from nearly normal to dramatically abnormal. The rod and cone components underlying the dark-adapted ERG photoresponses were estimated with the use of blue and red high-energy stimuli and a model of rod and cone phototransduction activation fit to the leading edges of the responses. Results from P2, P10, and P5 illustrate the range of results encountered (Fig. 4A). Maximum amplitude and sensitivity parameters of the phototransduction model summarize the rod and cone activation results (Fig. 4B). Assuming cross-sectional results in members of family 1 reflect different disease stages, the earliest (mildest) abnormality is reduction of rod maximum amplitude (P2, P3). The next disease stage may involve more loss of rod maximum amplitude and a reduction of cone sensitivity (P1, P10). Progression of disease is associated with further reductions of rod and cone maximum amplitude, with or without loss of sensitivity (P5, P7, P8, and P11). Results of ERG photo-

Table 1. Clinical Characteristics of the Patients

Mutation, Family, Patient	Age at Visit (y)/Sex	Visual Acuity*†	Kinetic Visual Field Extent†‡	Electroretinograms		
				Rod Amplitude§	Cone Flicker	
					Amplitude§	Timing
Arg677ter						
Family 1						
P1	10/F	20/20	88	34	55	N
	14	20/20	86	27	38	N
P2	31/M	20/20	100	N	N	N
P3	32/F	20/20	100	N	N	N
P4	32/M	20/20‖	80	ND	ND	ND
	33	20/20‖	67	np	np	np
	37	20/20‖	31	np	np	np
	43	20/20‖	15	np	np	np
P5	35/F	20/20	92	ND	25	Delay
P6	35/M	20/20	24	ND	4	Delay
P7	41/M	20/20	85	7	21	Delay
P8	43/F	20/20¶	83	ND	20	Delay
P9	51/F	20/30	76	ND	ND	ND
P10	53/F	20/20	96	33	42	N
P11	54/F	20/20	88	ND	12	Delay
Family 2						
P1	38/M	20/20	100	ND	27	Delay
P2	55/F	20/25	23	np	np	np
Family 3, P1	27/F	20/20	93	N	N	N
Family 4, P1	28/F	20/20	100	np	np	np
Family 5						
P1	31/F	20/20	75	np	np	np
	37	20/20	53	np	np	np
P2	53/M	20/25#	<1	np	np	np
	72	20/50#	<1	np	np	np
Family 6, P1	71/M	20/30	77	2	11	Delay
Family 7, P1	49/F	20/20	100	17	72	Delay
Family 8, P1	46/M	20/20	100	10	13	Delay
Family 9, P1	35/M	20/20	47	ND	ND	ND
Family 10, P1	32/M	20/15	100	8	9	Delay
Ser747 (1-bp del)						
Family 11						
P1	27/F	20/20	94	ND	ND	ND
P2	33/F	20/25	22	ND	3	Delay
P3	43/F	20/25	56	ND	ND	ND
	54	20/30	<1	np	np	np
Pro658 (1-bp ins)						
Family 12, P1	50/M	20/20	76	ND	67	Delay
Leu762-763 (5-bp del)						
Family 13, P1	64/F	20/20	90	ND	100	Delay
Tyr1053 (1-bp del)						
Family 14						
P1	31/M	20/20#	100	41	48	N
	47	20/20#	100	36	37	N
P2	86/F	20/100	<1	np	np	np

Patients with more than one listing underwent serial measurements. N, normal; ND, not detectable; np, not performed.

* Best corrected visual acuity.

† Similar in the two eyes, unless specified.

‡ Average of both eyes, expressed as a percentage of normal mean of V-4e target; 2 SD below normal equals 90%. This criterion was also used for IV-4e, if V-4e data were not available.

§ Percent of mean normal amplitude of participating ERG laboratories.

‖ 20/200, macular edema.

¶ Amblyopia, other eye.

<20/400, amblyopia, glaucoma.

responses recorded under light-adapted conditions were similar to those of the dark-adapted cones (not shown).

The relationship of rod to cone dysfunction was examined using ERG photoresponses (Fig. 4C) and dark-adapted psychophysics (Fig. 4D). Reduction of rod photoresponse maximum amplitude was always greater than the reduction of cone maximum amplitude (Fig. 4C). This result would be consistent with a greater retina-wide loss of outer segment membrane area in rods than in cones. Local rod–cone comparisons were performed with psychophysical methods. First, differences of sen-

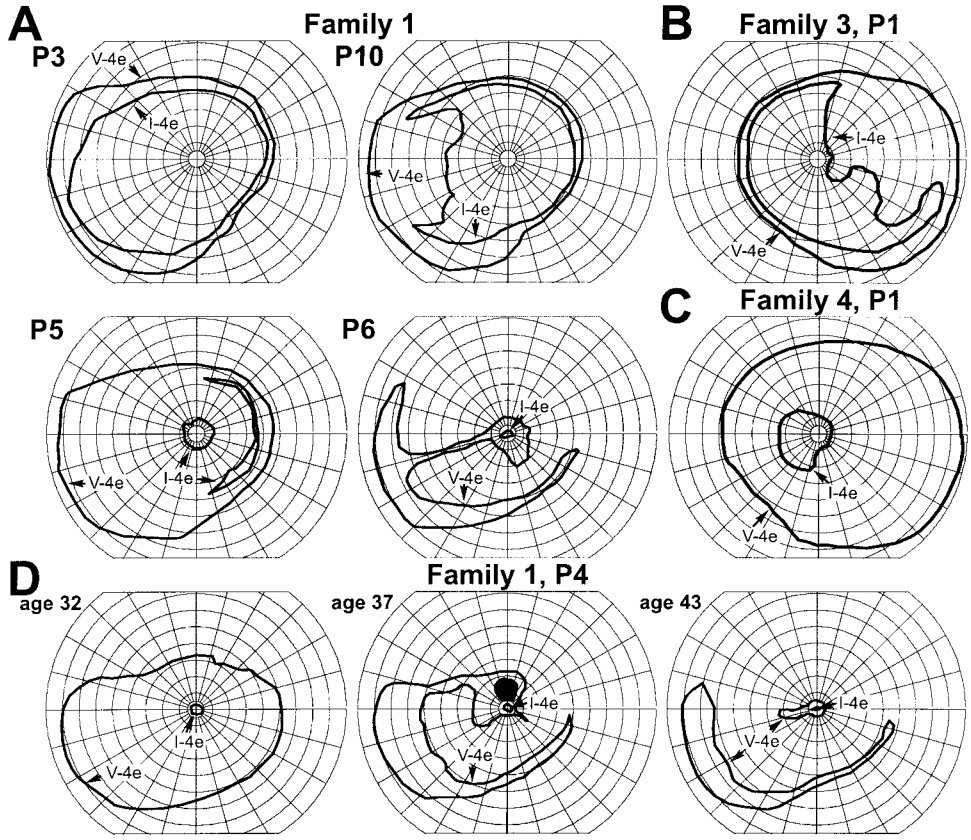

FIGURE 1. Kinetic visual fields in one eye of heterozygotes from three families with the Arg677ter *RP1* mutation (**A** through **C**). Serial results during an 11-year interval in one patient (family 1, P4) are shown (**D**).

sitivity to 500-nm and 650-nm stimuli (dark-adapted, 12° grid) were evaluated for spectral evidence of mediation by different photoreceptor types (mixed mediation, i.e., 500-nm stimulus being detected by rods and 650-nm stimulus by L/M cones[12]) Six patients (family 1: P5, P6, P7, P8, P10, P11) showed multiple (20, 7, 8, 17, 5, and 6, respectively) retinal loci with mixed mediation. At these loci, rods showed approximately 2 log units greater loss of sensitivity than cones (Fig. 4D). Mean field (72 loci on a 12° grid) loss of rod sensitivity to 500-nm stimuli (dark-adapted) was always greater than loss of cone sensitivity to 600-nm stimuli (light-adapted) in all patients (not shown).

Cross-sectional retinal images were used to gain understanding of "structural" change associated with dysfunction in three heterozygotes (family 1: P1, P2, and P4) with the Arg677ter *RP1* mutation. Central (toward superior) retinal scans of the three heterozygotes are displayed in gray scale (Fig. 5A) and then analyzed at two loci with LRPs (Fig. 5B). The gray scale displays suggest generalized retinal thinning outside the fovea in P1 and P4 versus P2. Analysis using LRPs demonstrates preservation of retinal structure at the fovea (I) with nearly identical waveforms in all three patients compared with normal. Of special interest is the outer retina–choroid complex (ORCC), the double-peaked structure in the scans. The first peak of the ORCC, believed to have origins in or near the photoreceptor inner and outer segments,[27,28] is preserved and is similar in normal and heterozygous subjects. These structural findings at the foveal locus are consistent with the functional findings of normal visual acuity (Table 1) and normal cone sensitivities (by dark- and light-adapted perimetry) at fixation in all three heterozygotes.

At the superior retinal locus (II), however, there was a marked difference in LRPs between heterozygotes. P2 had a waveform with the same overall thickness and subcomponents as normal individuals. Rod- and cone-mediated sensitivity was also normal at this locus. In contrast, P1 and P4 showed very abnormal OCT waveform shape. The abnormal features of these waveforms include reduced OCT thickness (from signal onset at vitreoretinal interface to offset of ORCC), loss of one of the two ORCC peaks, and increased reflectivity posterior to the ORCC (in P4). To understand these waveforms further, the signals have been cut and overlaid on parts of the normal template. The missing components in waveforms from P1 and P4 appear to be the valley preceding the ORCC and the first of the two ORCC peaks. These OCT features are believed to have origins in the outer nuclear layer and inner/outer segments, respectively.[27,28] Both P1 and P4 had visual dysfunction in the superior retinal region of OCT abnormality. P1 had one log unit of rod sensitivity loss, but no cone sensitivity loss, whereas P4 had no detectable function.

Phenotype of Other *RP1* Mutations

Heterozygotes with four different frameshift *RP1* mutations showed similarities in disease expression to that in patients with the Arg677ter mutation. In the age range from 27 to 64 years, six of seven patients studied retained at least 20/30 visual acuity and four of seven had 75% or more of normal kinetic field extent to a large target (Table 1). Visual fields in heterozygotes with a Leu762-763 (5-bp del), Pro658 (1-bp ins), or Tyr1053 (1-bp del) *RP1* mutations showed temporal and superior field losses (Figs. 6A, 6B, 6C). Rod ERG b-wave and cone flicker results suggested more rod than cone dysfunction

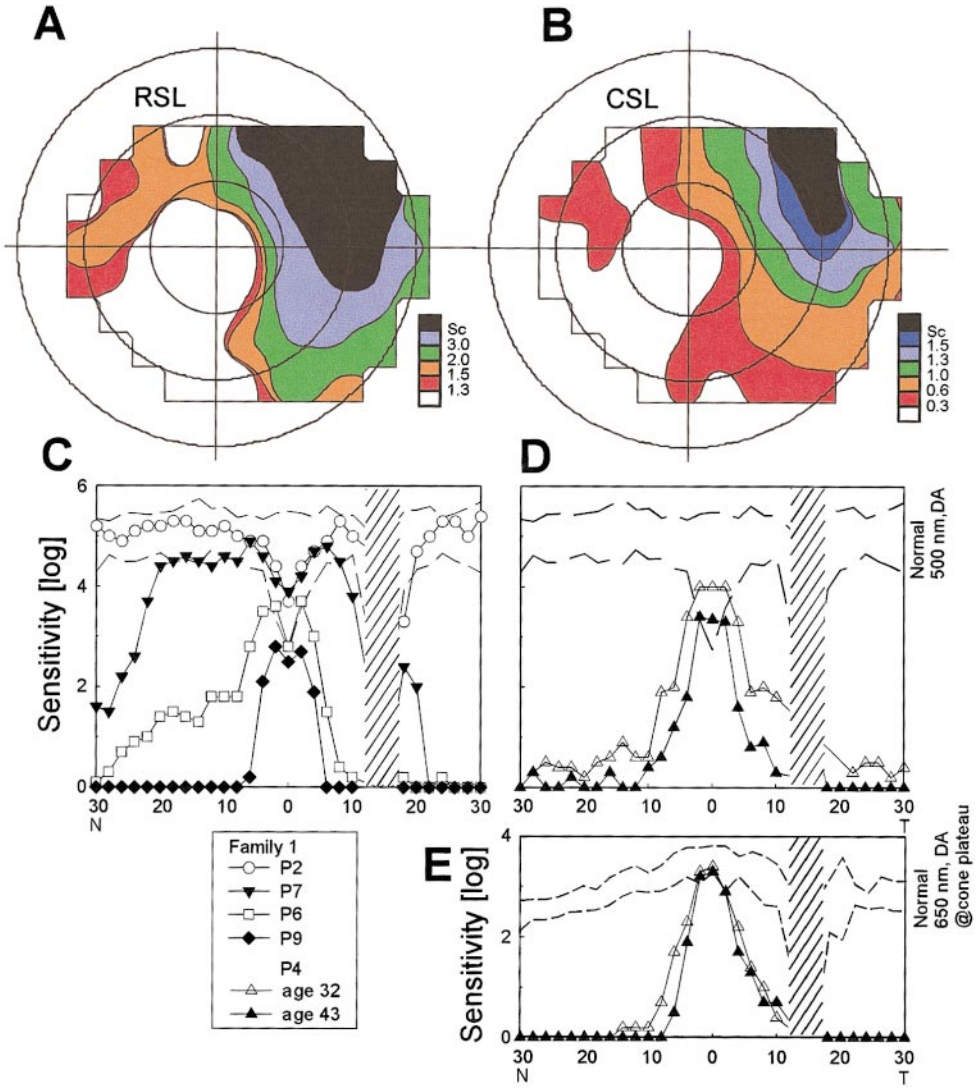

FIGURE 2. (**A**, **B**) Retinal topography of rod sensitivity loss (RSL) and cone sensitivity loss (CSL) summarized for seven mildly affected heterozygotes with Arg677ter *RP1* mutation from family 1 (P1, P5, P7–P11). RSL was measured with a 500-nm stimulus (dark-adapted) and CSL with a 600-nm stimulus (light-adapted). *Color transitions* depict the 50th percentile contour for a given level of sensitivity loss as specified (in log units) on the color scale (Sc, scotoma). Maps are shown as a visual field of the right eye. *Circles*: 20°, 40°, and 60° isoeccentricity lines; *irregular polygonal shapes*: extent of tested visual field. (**C, D,** and **E**) Dark-adapted sensitivity profiles across the horizontal meridian measured with 500-nm (**C**, **D**) and 650-nm (**E**) stimuli in family 1 members. All data depicted are from the right eye. *Dashed lines* represent limits (mean ±2 SD) of normal sensitivity obtained under dark-adapted conditions (**C**, **D**) or during the cone plateau period after a 99% bleach (**E**). *Hatched bar* marks the location of the physiological blind spot. N, nasal field; T, temporal field.

in the patients with Leu762-763 (5-bp del) or Pro658 (1-bp ins) mutations, whereas the heterozygote with the Tyr1053 (1-bp del) mutation showed relatively equal dysfunction in these ERG parameters. An older heterozygote in the latter pedigree (family 14, P2) was limited to only a central island of function with reduced visual acuity (Table 1; Fig. 6C).

All three heterozygotes with the Ser747 (1-bp del) *RP1* mutation had a generalized loss of visual function on kinetic perimetry (Fig. 6D) and severe retinal disease effects by ERG criteria (Table 1). Both the younger patients (ages 27 and 33) and their mother (at first examination, age 43) had no detectable rod ERG b-waves and little or no detectable cone flicker signals. Rod and cone sensitivities in the central 60° were measured in all three heterozygotes with the Ser747 (1-bp del) *RP1* mutation (Fig. 6E). Central rod function was measurable even when only a central island of vision remained (P3, age 54). At loci (on the 12° grid) with spectral evidence of mixed rod and cone mediation, there was consistently greater rod than cone dysfunction (Fig. 6F). Of interest, ophthalmoscopy in all seven patients with frameshift mutations showed pigmentary retinopathy that was more pronounced in the nasal than temporal retina.

DISCUSSION

Chromosome 8–linked RP in general and the Arg677ter mutation of the *RP1* gene specifically are now considered to be a relatively common form of adRP.[1,2,6] Our *RP1* gene screening, both targeted and of the entire gene, in a large cohort of

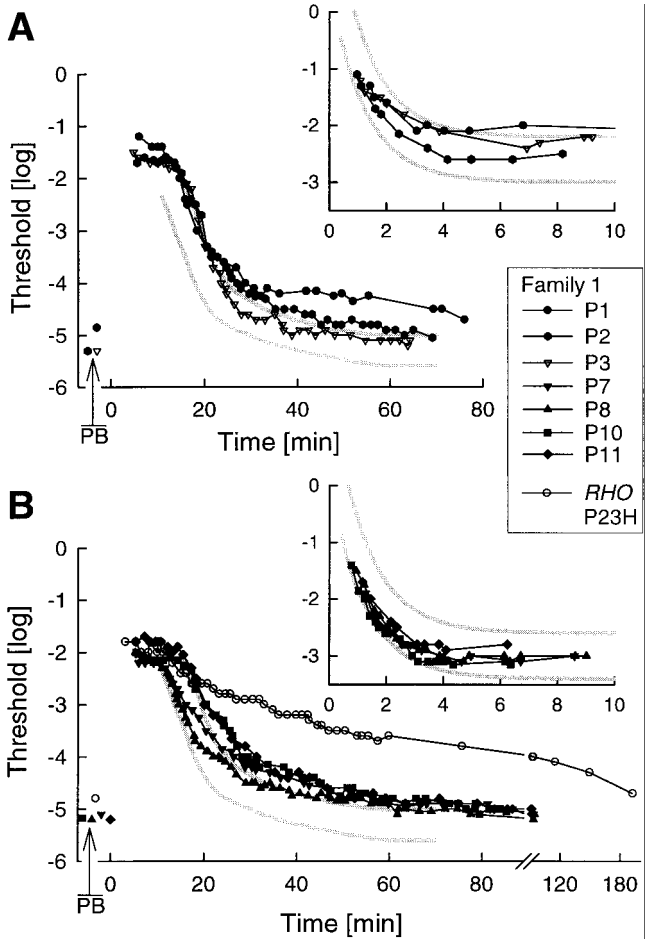

FIGURE 3. Dark adaptation tested at 34° in the inferonasal field (**A**) or at 12° inferior field (**B**) in members of family 1 with the Arg677ter *RP1* mutation. Prebleach (PB) thresholds were measured under fully dark-adapted conditions with a 500-nm stimulus. Time 0 corresponds to the end of light exposure that is expected to bleach 99% of the available visual pigment. Recovery of sensitivity was measured with a 650-nm stimulus (**A**, **B**: *insets*) during the initial 6 to 10 minutes and with a 500-nm stimulus (**A**, **B**) from 5 to 6 minutes until it reached within 0.1 log unit of PB thresholds. Dark adaptation results of a patient with adRP due to the P23H *RHO* mutation are shown for reference (○). Pairs of *solid gray lines* delimit the normal ranges.

probands clinically diagnosed as simplex, multiplex, autosomal recessive, or autosomal dominant RP confirms the previous observation that *RP1* mutations mainly cause adRP.[6] Two homozygotes for the Arg677ter mutation have been found in the large adRP UCLA-RP01 pedigree,[2] mirroring the rare finding of homozygosity for certain *RHO* mutations in consanguineous families.[30] In reports to date, disease-causing *RP1* mutations have all been in exon 4, clustering between codons 677 and 777, and lead to premature termination codons that are predicted to truncate the 2156–amino acid RP1 molecule.[1–3,6] Three of the four frameshift mutations in the current work are novel and extend the region of detected mutations in exon 4 from codons 658 to 1053. The Leu762-763 (5-bp del) *RP1* mutation has been noted before.[1,6]

The present study represents an early part of the quest for details of how *RP1* mutations lead to human retinal degeneration by studies of the heterozygous patients themselves. Currently, there are neither retinas obtained after death known to be from patients with *RP1* mutations nor studies in vitro or in animal models to draw on for details of disease mechanism.

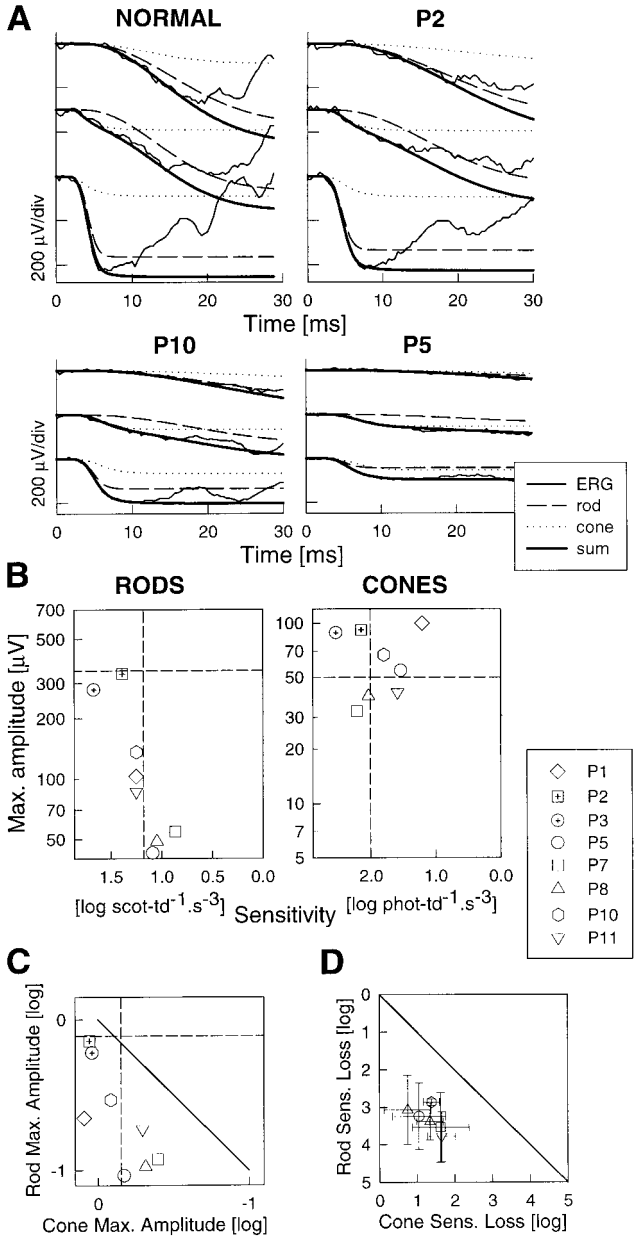

FIGURE 4. (**A**) Dark-adapted ERG photoresponses fit with a rod and cone phototransduction activation model in a representative normal subject and three patients. ERG photoresponses (*thin lines* in each panel) were evoked by a red (*middle*) and two blue (*top* and *bottom*) flash stimuli. Leading edges of the waveforms were fitted with a phototransduction activation model (*thick line*) that is the sum of rod (*dashed lines*) and cone (*dotted lines*) components. (**B**) Summary of rod and cone photoresponse parameters, maximum amplitude, and sensitivity, in eight patients; *dashed lines* are lower limits (mean −2 SD) of normal. (**C**) Comparison of rod and cone photoresponse maximum amplitudes. Data are plotted as the logarithm of the fraction of mean normal. *Dashed lines:* lower limits of normal; *solid line:* equal reduction of the two parameters. (**D**) Mean rod sensitivity loss as function of mean cone sensitivity loss at retinal loci where, under dark-adapted conditions, 500-nm stimuli were detected by rods and 650-nm stimuli were detected by cones. *Error bars:* 1 SD; n = 5–20. *Solid line:* equal reduction of the two parameters.

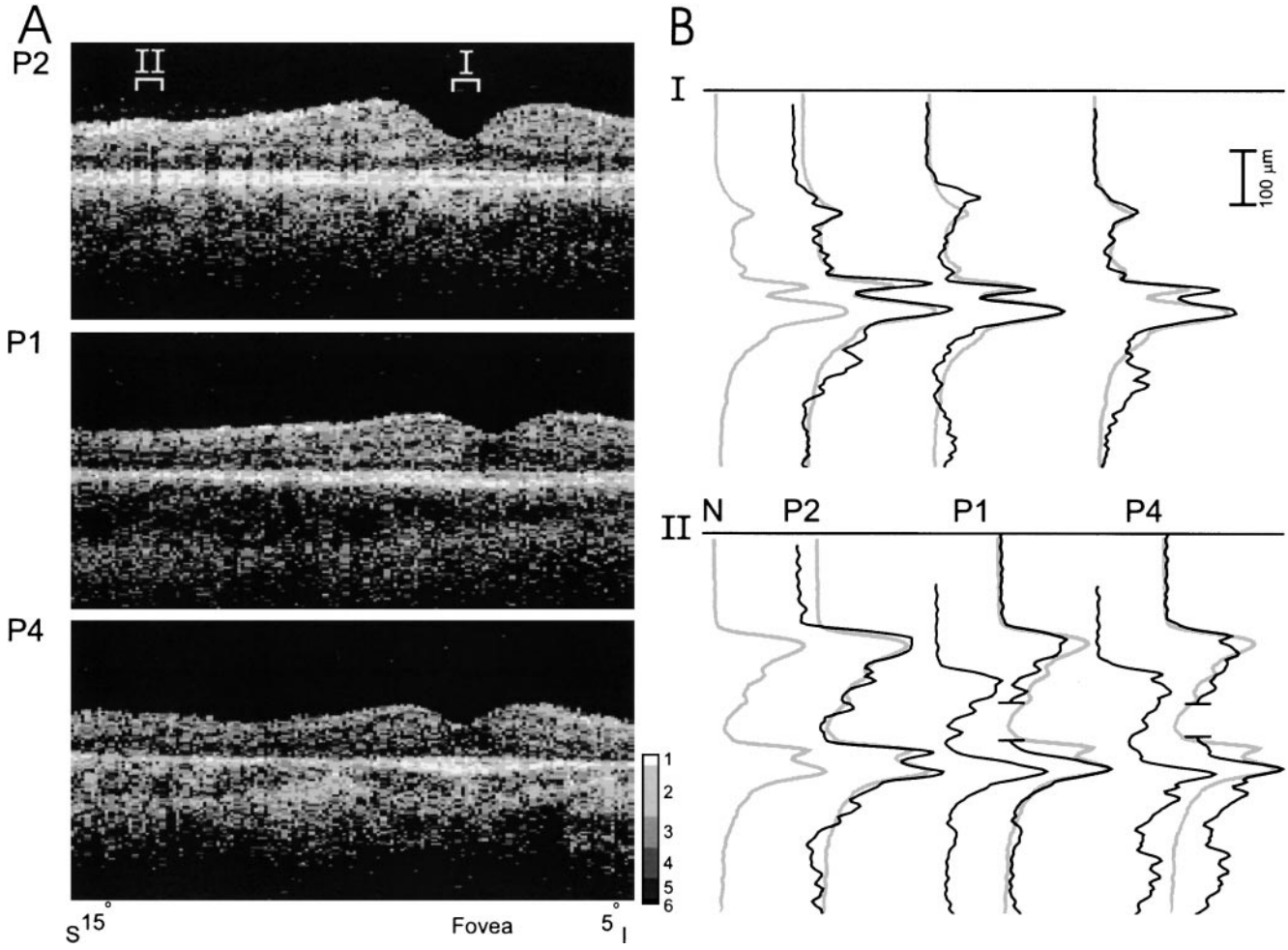

FIGURE 5. (**A**) Vertical OCT scans, from 15° superior (S) to 5° inferior (I) retina in three members of family 1. Sclera is toward the *bottom* of the figure; location of fovea is marked. OCT images are displayed with logarithm of reflectivity mapped to a gray scale (*lower right*). The numbers on the gray scale permit comparison of these OCT images with more commonly used pseudocolor displays (1, *white*; 2, *red*; 3, *yellow*; 4, *green*; 5, *blue*; and 6, *black*). (**B**) Comparison of longitudinal reflectivity profiles (LRPs) in three patients (*black* traces) and a representative normal subject (*gray* trace) from two locations (**A**: I, II). The LRPs of patients were aligned with normal by the last ORCC peak. Results from patients P1 and P4 at location II are shown twice: as original data (*left*) and as split data (*right*) to consider the hypothesis of missing retinal layers. Sclera is toward the *bottom*, and reflectivity signal increases toward the *right*. Depth calibration is shown at the *upper right*.

Mouse *Rp1* is expressed in photoreceptors,[1,3] but the exact localization and function of RP1 in human photoreceptors is not yet established.

RP1-associated disease has been briefly described in many molecular reports during the past two decades. In linkage studies of the extensive adRP UCLA-RP01 pedigree, now known to be caused by an Arg677ter *RP1* mutation,[1,2] it has been mentioned that the disease shows 1) night blindness in the second and third decades of life and "blindness by ages 45 to 60"[31,32]; 2) "diffuse retinal pigmentation, progressive decrease in recordable ERGs, concentric visual field loss," and two possible instances of incomplete penetrance[33]; and 3) "classic type 2 ADRP," defined as "regionalized and combined loss of rod and cone sensitivities on psychophysical testing."[34] An Australian adRP pedigree that mapped to 8q, was said to have a phenotype similar to UCLA-RP01.[35]

Recent molecular studies identifying the Arg677ter *RP1* mutation as the cause for UCLA-RP01 adRP reiterated these reports.[2] Ten other patients with this mutation were described as having "night blindness as an early symptom, constricted visual fields," visual acuities ranging from 20/20 to 20/70, and severely abnormal mixed and cone ERGs.[1] Other families with the Arg677ter *RP1* mutation have been said to show a more severe disease phenotype than that of UCLA-RP01 or the Australian pedigree. Nonpenetrance is mentioned to occur in one family.[6] Remarks have also been made about the phenotype of other *RP1* mutations. For example, it has been stated that "visual acuities and ERG findings (are) in the same range as patients with the Arg677ter mutation,"[1] or there is "mild disease with equal loss of rod and cone function,"[6] or "some families have mild disease . . . while others have more severe disease."[6]

There is a dearth of detail about early disease stages in all preceding work. We found that *RP1*-associated disease involves primarily rod photoreceptor function at the earliest stages. One of the more telling lines of evidence are the results from two mutation-positive heterozygotes in the fourth decade of life (family 1, P2, P3). These individuals would be considered examples of nonpenetrance by clinical examination but showed subtle abnormalities in rod ERG photoresponse max-

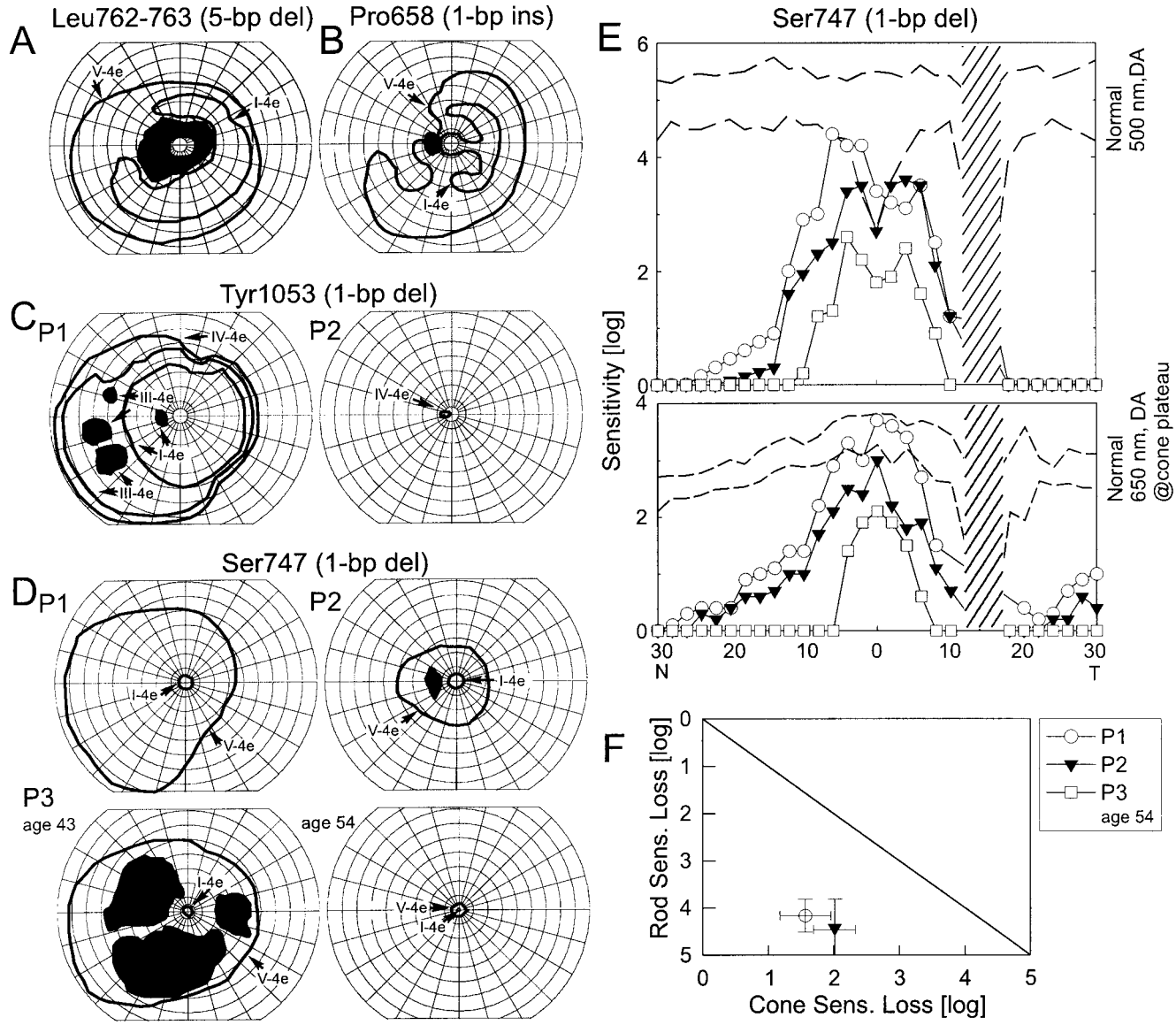

Figure 6. (**A** through **D**) Kinetic visual fields in one eye of heterozygotes from four families with different frameshift mutations in *RP1*. Results separated by an 11-year interval in one patient (family 11, P3) are also shown. (**E**) Dark-adapted sensitivity profiles across the horizontal meridian with 500-nm (*top*) and 650-nm (*bottom*) stimuli in three members of family 11. All data depicted are from the right eye. *Dashed lines:* limits (mean ±2 SD) of normal sensitivity obtained under dark-adapted conditions (*top*) or during the cone plateau period after 99% bleach (*bottom*). *Hatched bar:* physiological blind spot. N, nasal field; T, temporal field. (**F**) Mean rod sensitivity loss as function of mean cone sensitivity loss at retinal loci where, under dark-adapted conditions, 500-nm stimuli were detected by rods, and 650-nm stimuli were detected by cones. *Error bars:* 1 SD; n = 6 and 18. *Solid line* represents equal reduction of the two parameters.

imum amplitudes. These reductions of rod maximum amplitude would be consistent with retina-wide loss of rod outer segment membrane area (secondary to outer segment shortening and/or photoreceptor loss), albeit mild.

The disease in other patients with the *RP1* mutation we studied involved not only rods but also cones. There were reductions in cone ERG photoresponse maximum amplitudes, suggesting cone outer segment and/or cell losses. At all disease stages, ERG and psychophysical data indicated more rod than cone deficit. This is similar to the pattern found in dominant retinal degenerations caused by *RHO* mutations, but unlike many retinopathies associated with *RDS* mutations, which can show equal rod and cone losses.[22,36,37] In the patients studied who had the Arg677ter *RP1* mutation, we found loss of cone ERG photoresponse sensitivity. This can be explained as a reduction of gain during the activation phase of cone phototransduction. Reduction in cone sensitivity in RP of unknown genotype has been considered a secondary disease process due to decreased quantal catch, possibly from change in waveguide properties of cone outer segments distorted by loss of neighboring rods.[38] Our finding in some patients with Arg677ter *RP1* of loss of cone sensitivity but normal cone maximum amplitude (see Fig. 4B; P1, P5, and P10) is unusual.[38] Alternatively, RP1 may be more directly involved in the process of cone phototransduction.

There is a definite topography of disease predilection in the patients with *RP1* mutation whom we examined: A gradient of effect from most severe in the nasal and inferior retina to

least severe in the temporal and superior retina was evident. If not demonstrable on kinetic or static perimetry, it was observed on ophthalmoscopy in the patients studied. Previous reports of diffuse pigmentary retinopathy or concentrically constricted visual fields without mention of a pattern of loss suggest that patients in those reports may have been at later stages of disease than the patients in our investigation. The earliest detectable abnormalities in the vulnerable inferonasal retinal regions were rod-mediated sensitivity losses, but cone losses were also present in patients with more advanced disease.

Intraretinal differences in disease severity are not novel among adRP phenotypes.[30] In the era preceding molecular diagnosis, classification schemes of adRP identified many individuals and families with inferior retinal (superior field) abnormalities (for example, see References 39 and 40). The retinal topography of early *RP1* disease is reminiscent of that in patients with certain *RHO* gene mutations[14,30] but may not be exactly the same (compare current Fig. 2A with identically plotted contour maps in Reference 14, Fig. 3D). Some patients with class B1 *RHO* gene mutations (according to a recent scheme for classifying disease expression in *RHO* mutations[14]) clearly have inferior retina-wide (both nasal and temporal) defects, whereas many patients with *RP1* had defects almost confined to the nasal retina but more inferior than superior. Larger numbers of patients with *RP1* and class B1 *RHO* mutations must be examined to decide on the relationship between the two disease pathways. Are these only steps in a similar sequence of retinal degeneration or truly different intraretinal vulnerabilities? Of interest, patients with the *RP1* mutation, unlike class B1 patients with the *RHO* mutation, showed little or no prolongation of dark-adaptation kinetics. The association between the retinal disease gradient and prolonged adaptation in *RHO* mutations has led to speculation that a form of light damage due to chronic activation of rod photoreceptors could be a factor contributing to the degeneration.[14,41,42] In *RP1*, the two are not so associated, weighing against the light damage hypothesis as a generalizable mechanism. The retinal topography of *RP1* disease may result from regional differences in the expression of the *RP1* gene or currently unknown genetic or epigenetic factors that may interact with RP1 function.

The important issue of prognosis in *RP1* forms of adRP could not be investigated formally in the current cross-sectional study. For the central retina, however, functional and OCT structural evidence suggests longevity. Visual acuities remained near normal in most patients in our sample until late in life, although acuity in some patients became complicated by macular edema or other coincident ocular diseases. Preservation of visual acuity is consistent with other clinical data reported previously for *RP1* disease.[1] The normal-appearing central retinal OCT laminations attributable to photoreceptors[27,28] were consistent with functional data and in contrast to extrafoveal structure, which was severely altered in the two heterozygotes with reduced function in this region, presumably because of major loss of rods (and cones in family 1, P4).

Any diagnostic advice for families with *RP1* mutations must be tempered by the finding of substantial variability of disease severity, which seems to be a feature of the *RP1* form of adRP.[2] Highlighting this aspect of *RP1*-associated disease are the two Arg677ter *RP1* heterozygotes (family 1, P2, P3) who were not only asymptomatic but also would be considered normal by clinical criteria. In such patients at 50/50 risk of inheriting an *RP1* gene mutation, molecular diagnosis has to be the most certain method for detection. The intrafamilial and possibly interfamilial[6] differences in severity suggest that genetic and nongenetic risk factors may be involved in *RP1* disease expression. One potential factor already mentioned in relation to *RP1* gene expression has been oxygen sensitivity.[1] There is evidence for oxygen regulation of murine *Rp1* (along with other retinal genes): specifically, stimulation of expression by hypoxia and suppression by hyperoxia.[1] Interestingly, a complex role for oxygen in retinal degeneration was recently found in the *rdy* or Royal College of Surgeons (RCS) rat. Depending on disease stage, varying oxygen levels could have either positive or negative effects.[43] Determining the relationship between *RP1* disease expression and environmental or genetic modifiers is important, considering that it could lead to understanding the basis of the variable penetrance and even provide an opportunity for therapeutic intervention in this form of RP.

Acknowledgments

The authors thank K. Vandenburgh, T. Aleman, J. Huang, Y. Huang, M. Sharma, D. Marks, L. Gardner, E. DeCastro, J. Emmons, L. Streb, J. Andorf, D. Hanna, M. Benegas, and B. Koernig for their critical help with these studies; and J. Heckenlively for generous advice and sharing of data.

References

1. Pierce EA, Quinn T, Meehan T, McGee TL, Berson EL, Dryja TP. Mutations in a gene encoding a new oxygen-regulated photoreceptor protein cause dominant retinitis pigmentosa. *Nat Genet.* 1999;22:248–254.
2. Sullivan LS, Heckenlively JR, Bowne SJ, et al. Mutations in a novel retina-specific gene cause autosomal dominant retinitis pigmentosa. *Nat Genet.* 1999;22:255–259.
3. Guillonneau X, Piriev NI, Danciger M, et al. A nonsense mutation in a novel gene is associated with retinitis pigmentosa in a family linked to the RP1 locus. *Hum Mol Genet.* 1999;8:1541–1546.
4. Inglehearn CF. Molecular genetics of human retinal dystrophies. *Eye.* 1998;12:571–579.
5. Rattner A, Sun H, Nathans J. Molecular genetics of human retinal disease. *Ann Rev Genet.* 1999;33:89–131.
6. Bowne SJ, Daiger SP, Hims MM, et al. Mutations in the *RP1* gene causing autosomal dominant retinitis pigmentosa. *Hum Mol Genet.* 1999;8:2121–2128.
7. Inglehearn CF, McHale JC, Keen TJ, Skirton H, Lunt PW. A new family linked to the *RP1* dominant retinitis pigmentosa locus on chromosome 8q. *J Med Genet.* 1999;36:646–648.
8. Bassam BJ, Caetano–Anolles G, Gresshoff PM. Fast and sensitive silver staining of DNA in polyacrylamide gels. *Ann Biochem.* 1991; 196:80–83.
9. Weleber RG, Tobler WR. Computerized quantitative analysis of kinetic visual fields. *Am J Ophthalmol.* 1986;101:461–468.
10. Jacobson SG, Yagasaki K, Feuer WJ, Roman AJ. Interocular asymmetry of visual function in heterozygotes of X-linked retinitis pigmentosa. *Exp Eye Res.* 1989;48:679–691.
11. Grover S, Fishman GA, Brown J Jr. Patterns of visual field progression in patients with retinitis pigmentosa. *Arch Ophthalmol.* 1998; 105:1069–1075.
12. Jacobson SG, Voigt WJ, Parel J–M, Nghiem–Phu L, Myers SW, Patella VM. Automated light- and dark-adapted static perimetry for evaluating retinitis pigmentosa. *Ophthalmology.* 1986;93:1604–1611.
13. Jacobson SG, Kemp CM, Cideciyan AV, Macke JP, Sung C-H, Nathans J. Phenotypes of stop codon and splice site rhodopsin mutations causing retinitis pigmentosa. *Invest Ophthalmol Vis Sci.* 1994;35:2521–2534.

14. Cideciyan AV, Hood DC, Huang Y, et al. Disease sequence from mutant rhodopsin allele to rod and cone photoreceptor degeneration in man. *Proc Natl Acad Sci USA.* 1998;95:7103–7108.
15. Jacobson SG, Kemp CM, Sung C-H, Nathans J. Retinal function and rhodopsin levels in autosomal dominant retinitis pigmentosa with rhodopsin mutations. *Am J Ophthalmol.* 1991;112:256–271.
16. Cideciyan AV, Pugh EN Jr, Lamb TD, Huang Y, Jacobson SG. Rod plateaux during dark adaptation in Sorsby's fundus dystrophy and vitamin A deficiency. *Invest Ophthalmol Vis Sci.* 1997;38:1786–1794.
17. Fishman GA, Fishman M, Maggiano J. Macular lesions associated with retinitis pigmentosa. *Arch Ophthalmol.* 1977;95:798–803.
18. Weleber RG. The effect of age on human cone and rod Ganzfeld electroretinograms. *Invest Ophthalmol Vis Sci.* 1981;20:392–399.
19. Peachey NS, Fishman GA, Derlacki DJ, Alexander KR. Rod and cone dysfunction in carriers of X-linked retinitis pigmentosa. *Ophthalmology.* 1988;95:677–685.
20. Weleber RG, Eisner A. Retinal function and physiological studies. In: Newsome DA, ed. *Retinal Dystrophies and Degenerations.* New York: Raven Press; 1988:21–69.
21. Cideciyan AV, Jacobson SG. An alternative phototransduction model for human rod and cone ERG a-waves: normal parameters and variation with age. *Vision Res.* 1996;36:2609–2621.
22. Cideciyan AV. In vivo assessment of photoreceptor function in human diseases caused by photoreceptor-specific gene mutations. *Methods Enzymol.* 2000;316:611–626.
23. Huang D, Swanson EA, Lin CP, et al. Optical coherence tomography. *Science.* 1991;254:1178–1181.
24. Hee MR, Izatt JA, Swanson EA, et al. Optical coherence tomography of the human retina. *Arch Ophthalmol.* 1995;113:325–332.
25. Jacobson SG, Buraczynska M, Milam AH, et al. Disease expression in X-linked retinitis pigmentosa caused by a putative null mutation in the *RPGR* gene. *Invest Ophthalmol Vis Sci.* 1997;38:1983–1997.
26. Jacobson SG, Cideciyan AV, Huang Y, et al. Retinal degenerations with truncation mutations in the cone-rod homeobox (CRX) gene. *Invest Ophthalmol Vis Sci.* 1998;39:2417–2426.
27. Huang Y, Cideciyan AV, Papastergiou GI, et al. Relation of optical coherence tomography to microanatomy in normal and *rd* chickens. *Invest Ophthalmol Vis Sci.* 1998;39:2405–2416.
28. Huang Y, Cideciyan AV, Aleman TS, et al. Optical coherence tomography (OCT) in *rhodopsin* mutant transgenic swine with retinal degeneration. *Exp Eye Res.* 2000;70:247–251.
29. Kemp CM, Jacobson SG, Roman AJ, Sung C-H, Nathans J. Abnormal rod dark adaptation in autosomal dominant retinitis pigmentosa with proline-23-histidine rhodopsin mutation. *Am J Ophthalmol.* 1992;113:165–174.
30. Gal A, Apfelstedt–Sylla E, Janecke AR, Zrenner E. Rhodopsin mutations in inherited retinal dystrophies and dysfunctions. *Prog Retina Eye Res.* 1997;16:51–79.
31. Spence MA, Sparkes RS, Heckenlively JR, et al. Probable genetic linkage between autosomal dominant retinitis pigmentosa (RP) and amylase (Amy_2): evidence of an RP locus on chromosome 1. *Am J Hum Genet.* 1977;29:397–404.
32. Heckenlively J, Pearlman JT, Sparkes RS, et al. Possible assignment of a dominant retinitis pigmentosa gene to chromosome 1. *Ophthalmic Res.* 1982;14:46–53.
33. Daiger SP, Humphries MM, Giesenschlag N, et al. Linkage analysis of human chromosome 4: exclusion of autosomal dominant retinitis pigmentosa (ADRP) and detection of new linkage groups. *Cytogenet Cell Genet.* 1989;50:181–187.
34. Blanton SH, Heckenlively JR, Cottingham AW, et al. Linkage mapping of autosomal dominant retinitis pigmentosa (RP1) to the pericentric region of human chromosome 8. *Genomics.* 1991;11:857–869.
35. Xu S-Y, Denton M, Sullivan L, Daiger SP, Gal A. Genetic mapping of RP1 on 8q11–q21 in an Australian family with autosomal dominant retinitis pigmentosa reduces the critical region to 4 cM between D8S601 and D8S285. *Hum Genet.* 1996;98:741–743.
36. Jacobson SG, Cideciyan AV, Kemp CM, Sheffield VC, Stone EM. Photoreceptor function in heterozygotes with insertion or deletion mutations in the *RDS* gene. *Invest Ophthalmol Vis Sci.* 1996;37:1662–1674.
37. Jacobson SG, Cideciyan AV, Maguire AM, Bennett J, Sheffield VC, Stone EM. Preferential rod and cone photoreceptor abnormalities in heterozygotes with point mutations in the *RDS* gene. *Exp Eye Res.* 1996;63:603–608.
38. Hood DC, Birch DG. Abnormalities of the retinal cone system in retinitis pigmentosa. *Vision Res.* 1996;36:1699–1709.
39. Massof RW, Finkelstein D. Two forms of autosomal dominant primary retinitis pigmentosa. *Doc Ophthalmologica.* 1981;51:289–346.
40. Fishman GA, Alexander KR, Anderson RJ. Autosomal dominant retinitis pigmentosa: a method of classification. *Arch Ophthalmol.* 1985;103:366–374.
41. Heckenlively JR, Rodriguez JA, Daiger SP. Autosomal dominant sectoral retinitis pigmentosa. *Arch Ophthalmol.* 1991;109:84–91.
42. Li Z-Y, Jacobson SG, Milam AH. Autosomal dominant retinitis pigmentosa caused by the threonine-17-methionine rhodopsin mutation: retinal histopathology and immunocytochemistry. *Exp Eye Res.* 1994;58:397–408.
43. Valter K, Maslim J, Bowers F, Stone J. Photoreceptor dystrophy in the RCS rat: roles of oxygen, debris, and bFGF. *Invest Ophthalmol Vis Sci.* 1998;39:2427–2442.